ELSEVIER

Journal of Photochemistry and Photobiology A: Chemistry 97 (1996) 65–72

Journal of PHOTOCHEMISTRY AND PHOTOBIOLOGY A: CHEMISTRY

Effects of surface etching on the structure and performance of Rh_2O_3/CdS catalyst

Gongxuan Lu, Shuben Li *

State Key Laboratory for Oxo Synthesis and Selective Oxidation, Lanzhou Institute of Chemical Physics, Chinese Academy of Sciences, Lanzhou 730000, People's Republic of China

Received 22 August 1995; accepted 9 January 1996

Abstract

The effect of heat treatment at high temperature and etching with acetic acid on the composition, oxidation state and photoactivity of RhO_x/CdS catalysts was investigated. Our results indicate that heat treatment at high temperature is a crucial step in the enhancement of the photocatalytic activity of RhO_x/CdS catalysts, and they confirm the oxidation of $RhCl_3$ into Rh_2O_3 during heat treatment at 773 K in air (X-ray diffraction (XRD) and X-ray photoelectron spectroscopy (XPS) observations). Our results also indicate the formation of CdO, $CdSO_4$ and $CdCl_2$ during treatment at 773 K and their removal by washing with acetic acid solution at pH 4.5. The photoactivity results reveal that the pretreated catalyst exhibits a much higher activity for hydrogen generation from H_2S decomposition and methanol dehydrogenation on visible light irradiation. CdO shows no photoactivity regardless of the method used to prepare the catalyst. No evidence of $Cd(OH)_2$ or Rh_2S_3 formation was found in our investigation. XPS data suggest that there is a strong interaction between Rh_2O_3 and CdS after heating at 773 K. The possible mechanism of enhanced photocatalytic activity is discussed.

Keywords: Performance; Rh_2O_3/CdS catalyst; Structure; Surface etching

1. Introduction

Many different semiconductors have been used as photocatalysts for light-induced electron transfer reactions. CdS has attracted a great deal of attention because of its low band gap (2.4 eV) strong reducing ability of its conduction band (-0.9 V vs. saturated calomel electrode (SCE)) and strong oxidizing ability of its valence band hole (1.5 V vs. SCE) [1,2]. Noble metal loading can promote its light-induced electron transfer reactions [3–5]. CdS loaded with Rh_2O_3 has been shown to produce oxygen on illumination with visible light in the presence of $PtCl_6^{2-}$ as electron scavenger [6a]. Its activity was found to be superior to that of RuO_2/CdS in alkaline conditions [6b,c]. More recently, Rh_2O_3/CdS has also been used for the light-driven cleavage of hydrogen sulphide and the dehydrogenation of methanol [7–11].

In the preparation of highly active Rh_2O_3/CdS catalysts, heating in air at 300 °C for several hours, followed by an increase in temperature to 500 °C for 10 min, are important. Some workers have ascribed this to the complete conversion of $RhCl_3$ into Rh_2O_3 [6–12]. Etching with 0.2 M acetic acid (pH 4.5) is also very important, during which any CdO fraction which is present as a contaminant or is formed during heating in air at elevated temperatures can be removed from the surface of the CdS particles.

Although active M/CdS photocatalysts have been obtained by this method, the detailed mechanism is unknown. The purpose of this study is to provide detailed information on the effect of redox etching pretreatment on the control of the surface component and on the promotion of electron transfer reactions on the catalyst surface. The surface oxidation states of Rh and the photocatalytic activities are correlated. The possible mechanism of high temperature treatment is presented.

2. Experimental section

2.1. Materials

Cadmium sulphide (better than 99.999%) and $RhCl_3.H_2O$ (analytically pure grade) were purchased from Shanghai First Reagent Plant. All other chemicals were of at least analytically pure grade and were used as supplied. Double distilled water was used throughout.

* Corresponding author.

PII S1010-6030(96)04309-2

2.2. Photocatalyst preparation

Method A: CdS (2 g) was mixed thoroughly with the required amount of solution of $RhCl_3.H_2O$ (0.5 wt.% of $RhCl_3$); the slurry was dried at 353 K in air for 1 h, and subsequently heated in an oven at 573 K in air for 3 h.

Method B: the same treatment as described in method A was applied, followed by a rapid increase in temperature to 773 K which was maintained for 10 min; after this, the mixture was taken out of the oven and cooled to room temperature.

Method C: RhO_x loaded CdS, obtained from method B, was suspended in acetic acid solution at 333 K (pH 4.5) for 30 min, and then washed with distilled water and dried.

Method D: the same treatment as described in method B was applied except that the amount of Rh loaded was 3 wt.%.

Method E: the catalyst obtained by method C was reduced in a hydrogen atmosphere at 823 K for 2 h.

2.3. Apparatus

Illumination experiments were carried out in visible light with a wavelength longer than 440 nm. The reactor system was equipped with a 10 cm water jacket and a 440 nm filter to remove IR and UV radiation respectively. The reactor was made of quartz glass. The photoactivity was determined by the measurement of hydrogen produced during irradiation. In each run, 25 mg of catalyst was dispersed in 25 ml of Na_2S or methanol solution at room temperature. The hydrogen evolved during the tests was monitored by gas chromatography with a 13x column. A TD detector was used with argon as carrier gas. Blank tests were performed in the same conditions.

2.4. Characterization methods

The X-ray diffraction (XRD) measurements were performed using a Rigaku D1 MAX-RB X-ray diffractometer. The X-ray photoelectron spectroscopy (XPS) and Auger electron spectroscopy (AES) data were measured with a PHI-550 multifunctional spectrometer (P-E Co., USA) using Mg Kα radiation (power, 320 W; energy, 1253.6 eV). The voltage of argon ion sputtering was 4 kV, and the sputtered area was 5 mm × 5 mm. The binding energy was calibrated using the C 1s line of the sample (E_b = 284.6 eV). The error in the binding energy measurement was approximately 0.1 eV. Gas desorption mass spectra (GDMS) were obtained using a self-assembled quadrupole mass spectrometer connected to a multifunctional spectrometer. Transmission electron microscopy (TEM) and scanning electron microscopy (SEM) results were obtained using a JEM-7 electron microscope (Japan). The specific surface area data of the RhO_x/CdS catalysts were determined by a volumetric Brunauer–Emmett–Teller (BET) method with nitrogen as adsorbent.

3. Results

3.1. Characterization of Rh_2O_3/CdS photocatalysts

Commercial cadmium sulphide powder contains a certain amount of cadmium oxide [12]. CdO is formed by the slow oxidation of CdS in air. High temperature treatment in air promotes this oxidation process. No remarkable colour change occurs after 3 h thermal treatment at 573 K in air. However, subsequent heating at 773 K yields a dark yellow product. After etching, the colour of the catalyst is yellow–green. As shown by our XRD results in Fig. 1, the amount of CdO increases significantly after 10 min air treatment at 773 K, but not in the sample heated at 573 K for 3 h. The fraction of $CdSO_4$ (as $3CdSO_4.3H_2O$ and $CdSO_4.H_2O$) is also high after heating at 773 K. Washing these powders with acetic acid (pH 4.5) allows the dissolution of CdO and $CdSO_4$ without inducing significant dissolution of CdS itself. From the results of Refs. [11] and [12], these observations indicate that CdO and $CdSO_4$ are almost exclusively present on the surface of the CdS microcrystals. No evidence of $Cd(OH)_2$ formation is observed from our XRD data (usually, water in

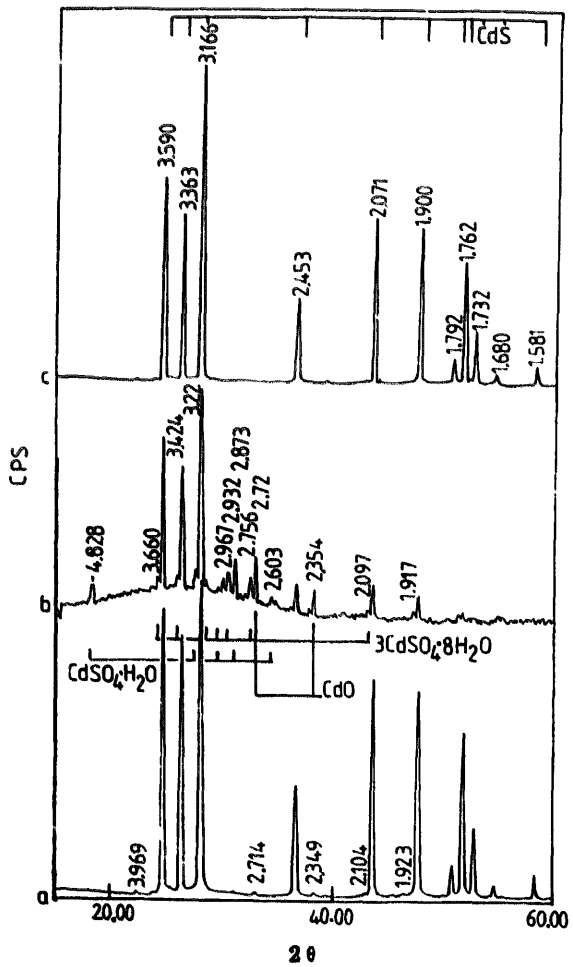

Fig. 1. XRD spectra of RhO_x/CdS catalysts: (a) catalyst A; (b) catalyst B; (c) catalyst C.

air is easily adsorbed by $CdSO_4$ and forms $CdSO_4.xH_2O$). It should be noted that $Cd(OH)_2$ can only be formed when CdO is mixed with KOH or NaOH [13] or in an aqueous dispersion at pH 10 [14]. No evidence of $CdCO_3$ formation is observed after treatment of catalyst B (because $CdCO_3$ will decompose into CdO and CO_2 at 573 K). Due to the small amount of $RhCl_3$ (approximately 0.5 wt.%), the XRD spectra show no signal for $CdCl_2$ formation. However, when the amount of $RhCl_3$ is increased to 20 wt.%, a clear signal of $CdCl_2$ is observed.

Heating at 573 or 773 K does not result in a significant change in the specific surface area of the catalyst (4.24 and 3.70 $m^2\ g^{-1}$ respectively); however, acetic acid etching results in a sharp decrease in the specific surface area (0.77 $m^2\ g^{-1}$). One possible reason for this is the elimination of the rough surface fractions of CdO and $CdSO_4$. It is observed by SEM that the edge sharpness of the CdS microcrystals increases after acetic acid etching. The particle size of this catalyst is around 1 μm and the RhO_x particle size on the CdS surface is about 3–5 nm (TEM results). No significant particle accumulation of RhO_x is observed during these treatments indicating that Rh_2O_3 is highly dispersed on the CdS surface.

In order to investigate the oxidation state of the surface components, the X-ray photoelectron spectra of the three different catalysts A, B and C were measured. The results are given in Fig. 2. Two peaks of S 2p are observed for catalyst A heated at 573 K for 3 h. The different strengths of the two peaks indicate that one kind of S species dominates the other on the surface of catalyst A. However, for catalyst B, heated at 773 K for 10 min, the strengths of the two S signals are almost the same. This indicates that the amounts of the two S species on the surface of catalyst B are roughly the same. After etching with acetic acid, only one S 2p peak remains. The signal at the high energy end represents the SO_4^{2-} species; therefore the results given above indicate SO_4^{2-} formation during high temperature heat treatment in air. This process is rather slow at 573 K but fast at 773 K (or near 773 K). No evidence of SO_4^{2-} species in catalyst C indicates that this oxidation process only occurs on the CdS surface, and not in the deep lattice phase (core structure), because oxygen diffusion in these conditions is slow.

A very significant segregation of chlorine species is observed in the high temperature heat treated sample. Since the amount of $RhCl_3$ is low (approximately 0.5 wt.%), and no XRD signal for the $CdCl_2$ phase is observed, the chlorine signal reveals that the chlorine species are formed mainly on the catalyst surface and can be removed easily by acetic acid etching.

There is no clear signal of Rh 3d in catalyst B, but strong signals in catalysts A and C. Only after etching with acetic acid can clear Rh 3d spectra be obtained. This indicates that the RhO_x species are formed near the inner CdS surface. Fig. 3 shows the X-ray photoelectron spectra as a function of the sputtering time with an argon beam for catalyst D; 3 wt.% of $RhCl_3$ was loaded on this sample in order to obtain clear

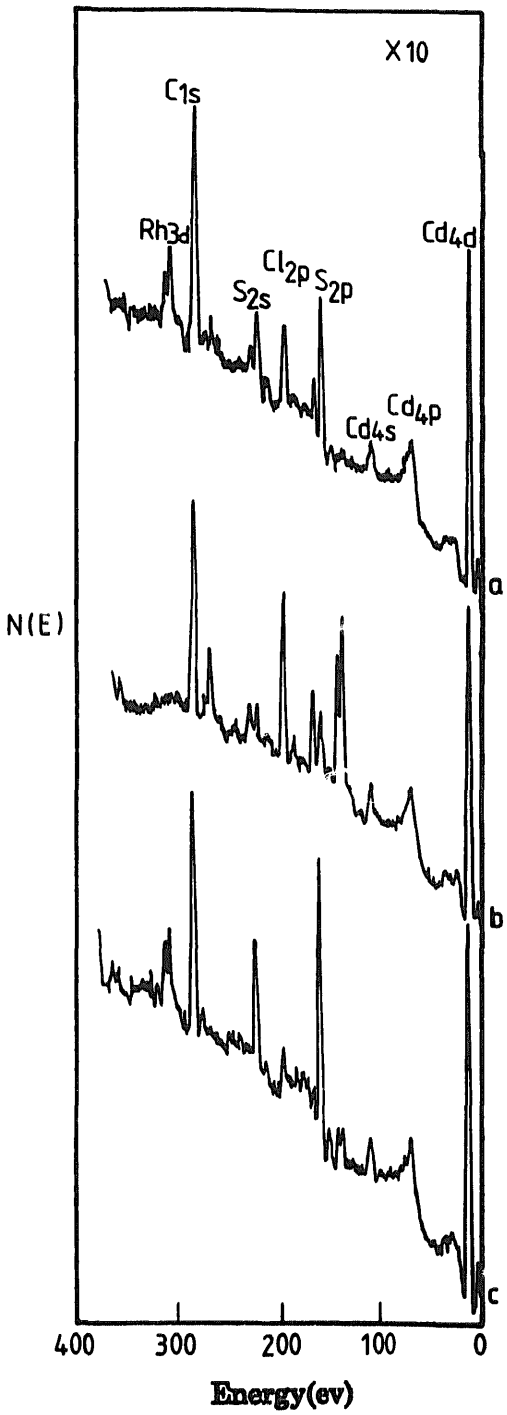

Fig. 2. X-Ray photoelectron spectra of RhO_x/CdS catalysts: (a) catalyst A; (b) catalyst B; (c) catalyst C.

spectra of Rh 3d. Before sputtering, the catalyst was heated at 573 K for 3 h and then at 773 K for 10 min. The sputtering area was 5 mm × 5 mm and the sputtering voltage was 4 kV. Initially, the C 1s and Cl 2p signal strengths decrease continuously as a function of the sputtering time. After 90 min sputtering, no clear C 1s and Cl 2p signals are observed, whereas the signals of S 2s, S 2p, Cd 4s and Cd 4d have increased. In addition, only one peak of S 2s remains after

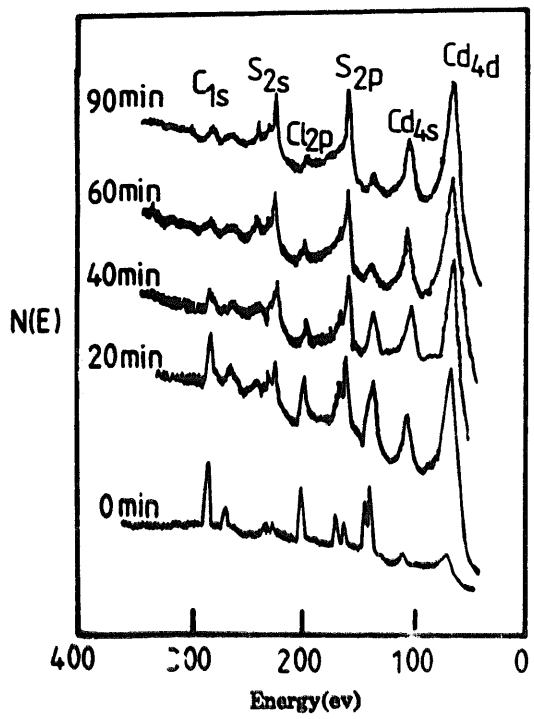

Fig. 3. X-Ray photoelectron spectra of catalyst D at different sputtering times. Sputtering conditions: 5 mm×5 mm, 4 kV, argon beam, 3 wt.% Rh_2O_3.

sputtering, which means that the adsorbed C, outer-surface chlorine and S^{6+} species have been sputtered away.

Since the outer-surface fraction will provide a large attenuation of the XPS signals, if several different cadmium components are distributed separately as a function of depth, the X-ray photoelectron spectra will mainly represent the outer cations. The signals of the buried cations will be attenuated relative to the signals of the cations on the surface. Furthermore, for some elements, such as Cd, the binding energy shift is very small and insufficient to determine the chemical situation. In this case, the Auger chemical shift of Cd exceeds the photoelectron chemical shift by approximately 4.9 eV [15]. Therefore we can obtain the exact chemical situation of Cd by comparing the binding energy and Auger line. The position of the Auger kinetic energy can be obtained by subtracting the Auger line from the photoenergy (Mg Kα, 1253.6 eV).

Table 1 compares the signals observed for XPS and Auger electrons emitted by X-ray-excited Cd cations in the different catalysts. For catalysts A and C (treated at 573 K and 773 K after etching), no pronounced binding energy difference is observed. However, the binding energy of Cd $3d_{5/2}$ in catalyst B heated at 773 K in air without etching is shifted to the higher energy end by about 0.5 eV, i.e. 405.7 eV. This is approximately the same as the Cd $3d_{5/2}$ line of $CdCl_2$ (405.9 eV). This indicates that cadmium on the outer surface of catalyst B is in an oxidative environment. From a comparison between the data in Ref. [16] and our experiments, the main component on the surface of catalysts A and C is CdS. Although the M4N45N45 line of catalyst B is similar to that of $Cd(OH)_2$, the binding energy and $\alpha+h\nu$ data are very different. From our results, the most probable explanation is that $CdCl_2$ and $CdSO_4$ are formed on the CdS catalyst surface at high temperature in air. This hypothesis agrees well with the XRD results. Only at pH > 8 does significant hydrolysis of Cd^{2+} occur [14]. From electrophoretic mobility curves, Hayes et al. [14] found that the CdS surface was coated by $Cd(OH)_2$ at pH values greater than 10 and the isoelectric point of $Cd(OH)_2$ is at pH 10.5. In addition, from the results for catalyst D and sputtering experiments, $CdSO_4$ is present nearer to the surface than CdO. When $CdSO_4$ is sputtered off, the signals of CdO appear. It is possible that the outermost fraction is $CdCl_2$, followed by $CdSO_4$ or CdO, and then Rh_2O_3 and CdS. The hydrogen reduction conditions promote $CdCl_2$ formation by passing through the chloride ions remaining after etching. This is understandable because CdS is easily reduced under an H_2 atmosphere to yield H_2S and $CdCl_2$.

The S 2p binding energy data of the different catalysts are shown in Fig. 4. The binding energy for S^{2-} and S^{6+} are 161.8 and 168.8–169.0 eV respectively in these catalysts. As expected, the S^{6+} signal is observed in catalyst A. This indicates the partial oxidation of CdS at 300 °C. However, the main fraction of this catalyst surface component is CdS (S^{2-}). In contrast, after heat treatment for a short time at 773 K in air, the S^{6+} signal increases sharply in catalyst B. Total oxidation of the outer surface of the catalyst is not observed as there is still a strong signal of S^{2-}. After washing with acetic acid at pH 4.5, the S^{6+} signal disappears in catalyst C, indicating the removal of the S^{6+} fraction (SO_4^{2-}). Sputtering experiments under ultrahigh vacuum (UHV) conditions also reveal that S^{6+} can be sputtered off easily. These results also suggest that the S^{6+} fraction only exists on the catalyst outer surface.

Table 1
Observed XPS and Auger signals for RhO_x/CdS prepared by different methods

Sample	Cd $3d_{5/2}$ (eV)	M4N45N45 (eV)	$\alpha+h\nu$ (eV)
CdS [16]	405.1	381.4	786.5
CdS [a]	405.3	380.5	785.8
CdS [b]	405.1	380.6	785.7
CdS [c]	404.9	380.9	785.8
CdO [16]	404.4	382.5	786.5
$Cd(OH)_2$ [16]	404.9	380.2	785.1
$CdCl_2$	405.9	379.9	785.8
$CdSO_4$	405.1	379.3	784.4
Catalyst A	405.2	381.4	786.6
Catalyst B	405.7	380.2	785.9
Catalyst C	405.2	381.4	786.6
Catalyst D	405.3	380.0	785.3
Catalyst E	405.8	380.1	785.9
Catalyst D [d]	404.2	382.4	786.6

[a] Bare CdS in UHV chamber at room temperature.
[c] Bare CdS in UHV chamber at 573 K.
[c] Bare CdS in UHV chamber at 873 K.
[d] Catalyst D after sputtering at 4 kV (5 mm×5 mm for 60 min).

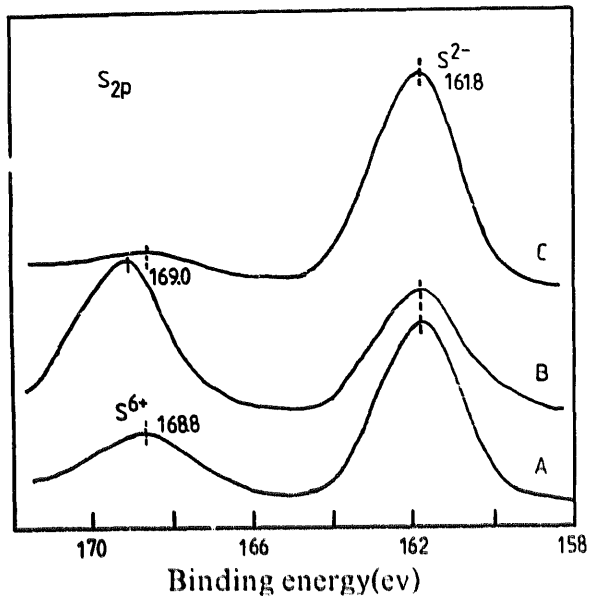

Fig. 4. S 2p spectra of different catalysts: (a) catalyst A; (b) catalyst B; (c) catalyst C.

Table 2
O 1s binding energy data of different catalysts and references

Sample	O 1s (eV)	Possible oxygen species
CdS	532.1	H_2O weakly adsorbed
CdS	531.8	H_2O tightly adsorbed
CdS	531.4	–OH hydroxyl
$RhCl_3$ on Au foil [a]	532.1	H_2O weakly adsorbed
$RhCl_3$ on Au foil [b]	531.4	–OH hydroxyl
$RhCl_3$ on Au foil [c]	529.8	Lattice O in RhO_x
$RhCl_3$ on Au foil [d]	529.7	Lattice O in Rh_2O_3
$RhCl_3$ on Au foil [e]	531.8	H_2O tightly adsorbed
Catalyst A	531.5	–OH hydroxyl
Catalyst B	531.8	H_2O tightly adsorbed
Catalyst C	531.5	–OH hydroxyl
Catalyst D	531.7	H_2O tightly adsorbed
Catalyst D [f]	528.5	Lattice O in CdO
	531.0	Lattice O in RhO_x

[a] $RhCl_3$ on Au foil at room temperature.
[b] $RhCl_3$ on Au foil after 3 h calcination at 573 K in air.
[c] $RhCl_3$ on Au foil after 3 h calcination at 773 K in air.
[d] $RhCl_3$ on Au foil after 3 h calcination at 1073 K in air.
[e] $RhCl_3$ on Au foil after 3 h calcination at 1073 K in air, then H_2 reduction at 823 K for 1 h.
[f] Catalyst D after sputtering at 4 kV (5 mm×5 mm for 60 min).

Investigations of the O 1s binding energy are very complex. The O 1s binding energy is dependent on the chemical situation of the oxygen atoms, the materials used and the apparatus. Thus it is not advisable to draw conclusions from X-ray photoelectron spectra only without other methods as reference. Several kinds of oxygen species exist on the catalyst surface: O from SO_4^{2-}, CdO, H_2O in the lattice of $CdSO_4 \cdot xH_2O$, adsorbed O_2, CO_2, H_2O, etc. In order to study this problem, highly pure CdS with no Rh was chosen to set up the O 1s line reference on the CdS surface. Both XPS and GDMS were used to identify the surface O components. H_2O desorption exhibits three main states of adsorbed H_2O. The H_2O desorption signal appears at room temperature and reaches the first maximum at 573 K and the second at 773 K. The signal at room temperature represents weakly adsorbed water, which is simply hydrogen bonded to surface S atoms; the peak at 573 K represents tightly adsorbed water, which is non- dissociative with the oxygen atom coordinated to a surface metal atom; the peak at 773 K represents the most tightly bound water which is dissociatively adsorbed as hydroxyl. Consequently, in considering the O 1s binding energies listed in Table 2, we can deduce that the O 1s line for weakly adsorbed water is 532.1 eV, the O 1s line for tightly adsorbed water is 531.8 eV and the O 1s line for the most tightly adsorbed water (as hydroxyl) is 531.4 eV.

Another important O 1s reference line is O 1s of RhO_x. In order to obtain these data, $RhCl_3$ was loaded onto Au foil and then calcined in air at different temperatures from 273 to 1073 K. As shown in Tables 2 and 3, Rh $3d_{5/2}$ of the sample calcined at 1073 K is 308.0 eV, which is identical to that of Rh $3d_{5/2}$ in Rh_2O_3. The corresponding O 1s line is equivalent to 529.7 eV. Therefore the main O species on the surface of catalysts A and C is dissociatively adsorbed hydroxyl, while the main O species on the surface of catalysts B and D is tightly adsorbed water. From the XRD results, this may be the lattice water in $CdCl_2.xH_2O$ or $CdSO_2.xH_2O$.

In order to determine the O species distribution with depth in catalyst D, argon ion beam sputtering was used to peel the shell of $CdSO_4$ and $CdCl_2$ until the Cd signal of CdO was observed. The O 1s lines of O in CdO and Rh_2O_3 are at 528.5 and 531.0 eV respectively (see Table 2). Therefore the component distribution with depth in catalysts B and D can be described as shown in Fig. 5.

In the investigation of $Rh_2O_3/SrTiO_3$ by Lehn et al. [17], the binding energy of Rh $3d_{5/2}$ in the catalyst obtained by

Table 3
Binding energies of different catalysts and references

Sample	Rh $3d_{5/2}$ (eV)	Possible Rh species
$RhCl_3$ on Au foil [a]	309.8	Rh in $RhCl_3$
$RhCl_3$ on Au foil [b]	309.3	Rh in RhO_xCl
$RhCl_3$ on Au foil [c]	308.	Rh in RhO_xCl
$RhCl_3$ on Au foil [d]	308.0	Rh in Rh_2O_3
$RhCl_3$ on Au foil [e]	307.4	Rh metal
Catalyst A	309.1	Rh in RhO_xCl
Catalyst B	307.6	Rh in Rh_2O_3
Catalyst C	307.2	Rh in Rh_2O_3
Catalyst D	306.6	Rh in Rh_2O_3
Catalyst E	307.0	Rh metal
Catalyst D [f]	306.6	Rh in Rh_2O_3

[a] RhCl on Au foil at room temperature.
[b] $RhCl_3$ on Au foil after 3 h calcination at 573 K in air.
[c] $RhCl_3$ on Au foil after 3 h calcination at 773 K in air.
[d] $RhCl_3$ on Au foil after 3 h calcination at 1073 K in air.
[e] $RhCl_3$ on Au foil after 3 h calcination at 1073 K in air, then H_2 reduction at 823 K for 1 h.
[f] Catalyst D after sputtering at 4 kV (5 mm×5 mm for 60 min).

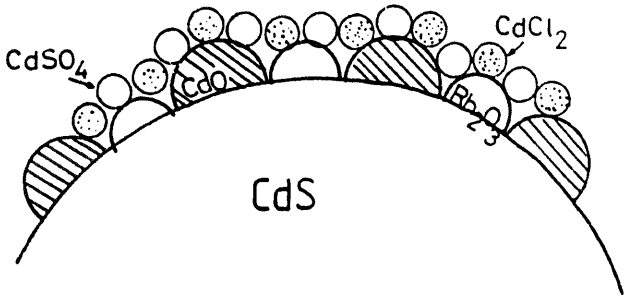

Fig. 5. Possible structure of catalysts B and D.

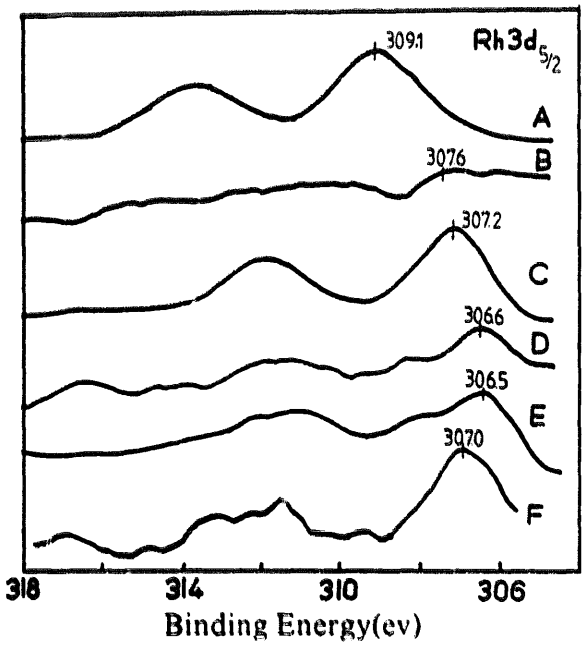

Fig. 6. Binding energy of Rh $3d_{5/2}$ of different catalysts: (A) catalyst A; (B) catalyst B; (C) catalyst C; (D) catalyst D; (E) catalyst D after 90 min sputtering at 4 kV, 5 mm×5 mm with argon beam; (F) catalyst C after reduction in H_2 at 823 K for 2 h.

heating at 773 K was nearly 309.3 eV. However, in the work by Li et al. [10], the binding energy of Rh $3d_{5/2}$ in Rh_2O_3/TiO_2 catalyst heated at 773 K was around 308.2 eV. These results indicate that the nature of loaded Rh_2O_3 on different semiconductors is quite different. In the present work, the binding energy of Rh $3d_{5/2}$ of Rh_2O_3/CdS treated at 773 K for 10 min is 307.2 eV (see Fig. 6), while that of RhO_x/CdS treated at 573 K for 3 h is 309.1 eV. In comparison with the data in Ref. [14], Rh $3d_{5/2}$ of the sample heated at 773 K is shifted to lower energy by nearly 1 eV. In another separate experiment, $RhCl_3$ was loaded onto Au foil. Treatments similar to the catalyst preparation processes given above were used and Rh $3d_{5/2}$ binding energies were obtained. The results are listed in Table 3 (Au 4f and C 1s lines used as references). Clearly, the binding energy of Rh $3d_{5/2}$ of $RhCl_3$ is 309.8 eV, while that of Rh_2O_3 is 308.0 eV. The data at 309.3 and 308.6 eV only represent partially oxidized $RhCl_3$. The binding energy of metallic Rh is 307.4 eV. There are two possibilities for the low Rh $3d_{5/2}$ data in catalysts C and D. During high temperature treatment, several possible reactions can occur in air as shown below

$$2RhCl_3 \cdot 3H_2O \longrightarrow Rh_2O_n(OH)_{3-n} + 6HCl \quad (1)$$

$$Rh_2O_n(OH)_{3-n} \longrightarrow Rh_2O_3 + 3/2H_2O \quad (2)$$

$$2RhCl_3 + 3CdS \longrightarrow Rh_2S_3 + 3CdCl_3 \quad (3)$$

$$Rh_2S_3 + O_2 \longrightarrow Rh + SO_2 \quad (4)$$

$$2HCl + CdS + O_2 \longrightarrow CdCl_2 + H_2O + 1/2SO_2 \quad (5)$$

$$CdS + 3/2O_2 \longrightarrow CdSO_3 \longrightarrow CdO + SO_2 \quad (6)$$

$$CdSO_3 + 1/2O_2 \longrightarrow CdSO_4 \quad (7)$$

The Rh $3d_{5/2}$, Cd $3d_{5/2}$ and S 2p binding energy data of the different catalysts are listed in Table 4. For the approximately pure surface of CdS (bare CdS desorbed in a UHV chamber at a temperature higher than 573 K), the Cd $3d_{5/2}$ binding energy is in the range 404.9–405.1 eV and that of S 2p is in the range 161.1–161.2 eV. The Cd $3d_{5/2}$ and S 2p binding energies of impregnated $RhCl_3$/CdS and hydrogen reduced catalyst E lie within these ranges, and the correspond-

Table 4
Rh $3d_{5/2}$, Cd 3d, S 2p and Cl 2p data of different catalysts and references

Sample	Cd 3d (eV)	S 2p (eV)	Cl 2p (eV)	Rh $3d_{5/2}$ (eV)	Rh/Cl
CdS [a]	405.2	161.3			
CdS [b]	405.1	161.2			
CdS [c]	404.9	161.1			
$RhCl_3$/CdS	404.9	161.0	197.9	309.9	1:3.12
Catalyst A	405.2	161.7	198.9	309.1	1:2.1
Catalyst B	404.5	161.6	198.8	307.2	1:1.16
Catalyst C	405.2	161.8	198.0	307.2	2.6:1
Catalyst E	405.1	161.3	198.3	306.6	1:2.7
$CdCl_2$	405.9	198.5			

[a] Bare CdS in UHV chamber at room temperature.
[b] Bare CdS in UHV chamber at 573 K.
[c] Bare CdS in UHV chamber at 873 K.

Table 5
Effect of pretreatment on the activity of RhO_x/CdS catalysts

Sample	Rate of hydrogen evolution (10^{-4} ml h^{-1} (mg cat)$^{-1}$)	
	In 0.1 M Na_2S (pH 12)	In 70% methanol–water (pH 12)
Catalyst A	0.35	0.95
Catalyst B	0.90	0.40
Catalyst C	3.35	2.75

ing Rh $3d_{5/2}$ data are in line with that of $RhCl_3$ and metallic Rh. However, after high temperature heat treatment above 573 K, the Cd $3d_{5/2}$ and S 2p binding energies are shifted to lower energies (see Table 4), especially for the samples treated at 773 K. These results may indicate the strong interaction of Rh_2O_3 and CdS in the Rh_2O_3/CdS catalyst treated at 773 K.

The GDMS results support this hypothesis and provide evidence for the determination of the surface reactions occurring during high temperature treatment. We used 20 wt.% $RhCl_3$/CdS as a model sample. After treatment at 573 K for 3 h, this sample was analysed by GDMS. The GDMS results are as follows: (1) between room temperature and 573 K, strong desorption signals of water and HCl are observed; however, the signals of oxygen and carbon dioxide desorption are low; (2) between 573 and 873 K, the signals of SO_2, HCl, O_2 and CO_2 desorption increase with increasing temperature, and the signals of SO_2, O_2 and CO_2 reach a maximum at 773 K. These results indicate that the oxidation of S atoms occurs simultaneously with HCl formation. After the GDMS experiments, the atomic concentration of Cl has decreased from 13.9% to 4.4%, while the atomic concentrations of S, O and Rh have increased from 11.5%, 24.6% and 3.1% to 18.3%, 29.3% and 5.6% respectively; this can be attributed to the formation and desorption of HCl, the oxidation of S and the formation of Rh_2O_3 and SO_2.

Is there any possibility of Rh metal formation passing through the sulphide compound? In order to check for this possibility, we prepared a model sample containing 20 wt.% $RhCl_3$ in 1 g of highly pure CdS. After treatment at 573 K for 3 h and at 773 K for 10 min, the colour of this mixture changed from yellow to dark green. This product was sent for XRD analysis. The results reveal that Rh_2O_3 is present in this sample. No evidence of metallic Rh or Rh_2S_3 formation is observed in the XRD spectra of the samples heated at 573 and 773 K. Therefore the low binding energy of Rh $3d_{5/2}$ in catalysts B and C does not represent Rh metal formation on the CdS surface after high temperature treatment, i.e. reactions (3) and (4) do not occur during our catalyst preparation process.

3.2. Photocatalytic activity of different catalysts

Table 5 shows the rate of hydrogen evolution on illumination of RhO_x/CdS catalyst dispersions with visible light. With S^{2-} as hole scavenger, hydrogen is formed according to

Cathode: $2H_2O + 2e^- \longrightarrow H_2 + 2OH^-$

Anode: $2S^{2-} + 2h^+ \longrightarrow S_2^{2-}$

where e^- and h^+ are produced in the conduction band and valence band respectively on visible light irradiation. The volume of hydrogen evolved is a linear function of the illumination time during our test. In 0.1 M Na_2S (pH 12), the activity of catalyst C is highest. The activity of catalyst B is higher than that of the unpretreated catalyst. The hydrogen formation rates of irradiated RhO_x/CdS catalyst dispersions in methanol–water (70% methanol, pH 12) are similar, but with a reverse order for catalysts A and B. However, catalyst C shows the highest photoactivity. This indicates that Rh_2O_3 loading on CdS promotes the redox reaction significantly, i.e. hydrogen evolution. CdO absorbs light up to 560 nm and acts as an optical filter of absorbed and emitted light [12]. Our results reveal that the catalytic activity decreases in the presence of CdO. Pure CdO and CdO obtained from $Cd(NO_3)_2$ exhibit no photoactivity for hydrogen production. Thus for the preparation of a good M/CdS catalyst, CdO must be eliminated.

4. Discussion

Two kinds of CdS structural type exist, i.e. cubic and hexagonal close-packed arrangement of the anions. In both structural types, tetrahedral T^+ (or T^-) sites are occupied and octahedral sites are empty. The interatomic distance in cubic or hexagonal CdS can be calculated from the unit cell dimensions [18], and these data are listed in Table 6. GDMS experiments reveal that tightly bonded hydroxyl desorbs at 773 K, while strongly adsorbed water desorbs at 573 K. However, for $RhCl_3$/CdS, the water desorption signals are continuously high between room temperature and 773 K. In addition, HCl is the main desorption product. This indicates that Rh_2O_3 is formed at the same time as the formation and desorption of water and HCl. It seems that physically adsorbed water has very little effect on the Rh_2O_3 loading. However, water bonded to metal atoms blocks the sites which would otherwise adsorb $RhCl_3$ (usually as $RhCl_3.3H_2O$ in water). Water

Table 6
Interatomic distances in CdS and Rh_2O_3 [18]

Structural type	Distance (Å)	
Cubic CdS	Cd–S	2.159
	Cd–Cd	4.113
	S–S	4.113
Hexagonal CdS	Cd–S	2.530
	Cd–Cd	4.130
	S–S	4.130
Rh_2O_3	Rh–O	2.05

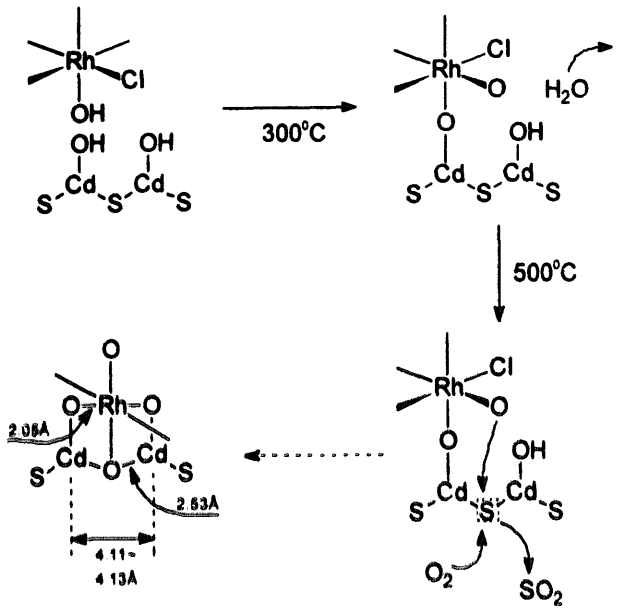

Fig. 7. Possible mechanism of high temperature treatment in air and related structure.

hydrogen bonded to the S atoms will desorb at 573 K. In this case, the Rh atom in $RhCl_3.3H_2O$ will link with an O atom of surface bonded hydroxyl by a condensation reaction when the impregnated catalyst is heated at 573 K. At the same time, HCl is formed and desorbs from the sample. When this sample is further heated at 773 K in air, surface S atoms will be oxidized to SO_2 and an S vacancy will form. The neighbouring S vacancy of the Cd atom will be occupied by a terminal O atom linked to an Rh atom. The terminal Cl atom linked to Rh and O atoms in the neighbouring hydroxyl can bond together and release a molecule of HCl. Indeed, strong desorption of SO_2 and HCl is observed during this treatment. In other words, $RhCl_3.3H_2O$ is converted into Rh_2O_3 by a condensation reaction and linked to the surface of CdS by an oxygen bridge. The structural data listed in Table 6 are in good agreement with this hypothesis. Thus this kind of structure results in a strong interaction between Rh_2O_3 and CdS, and provides a special path of electron transfer excited by visible light (see Fig. 7). The simultaneous process on bare CdS will involve the oxidation of CdS at 773 K. Our experimental evidence indicates that $CdSO_4$ and CdO are the oxidized products. HCl, formed by a condensation reaction, may also react with Cd to produce $CdCl_2$. These products can be removed by acetic acid at pH 4.5. This process produces a bare CdS surface and island-like Rh_2O_3 residing on the CdS surface; the former acts as a light absorption centre and the latter acts as an electron transfer centre; both are necessary for high activity performance. No evidence of $Cd(OH)_2$ formation is observed.

5. Conclusions

The results obtained in this paper verify that high temperature treatment at 773 K in air leads to $RhCl_3$ conversion into Rh_2O_3, which acts as a photoreaction centre. XPS results suggest that there is strong interaction between Rh_2O_3 and CdS in the Rh_2O_3/CdS system after high temperature treatment. XRD, XPS, AES and GDMS studies reveal that $CdSO_4$, $CdCl_2$ and CdO are formed during this high temperature treatment, and these components can be removed by etching with acetic acid at pH 4.5. No evidence for $Cd(OH)_2$ and Rh_2S_3 formation is observed. $CdCl_2$ and $CdSO_4$ exist only at the outer surface of catalysts B and D, while Rh_2O_3 is located near the CdS surface. The reasons for the high activity of the catalysts obtained by this method are as follows: (1) the formation of a bare CdS surface with island-like Rh_2O_3; the former acts as a light absorption centre and the latter acts as an electron transfer centre; (2) the strong interaction between Rh_2O_3 and CdS promotes charge transfer during the photoreaction.

References

[1] M.A. Grätzel (ed.), *Energy Resources through Photochemistry and Catalysis*, Academic Press, New York, 1983.
[2] T. Watanabe, A. Fujishima and K. Honda, *Chem. Lett.*, (1974) 897.
[3] D.H.M.W. Thewissen, A.H.A. Tinenemans, M. Eeuwhorst-Reinten, K. Timmer and A. Mackor, *Nouv. J. Chim.*, *7* (1983) 191.
[4] J.R. Darwent, *J. Chem. Soc., Faraday Trans. 2*, *77* (1981) 1703.
[5] J.R. Darwent and G. Porter, *J. Chem. Soc., Chem. Commun.*, (1981) 145.
[6] (a) N.M. Dimitrijevic, S.B. Li and M.A. Grätzel, *J. Am. Chem. Soc.*, *106* (1984) 6565; (b) A. Mills and G. Williams, *J. Chem. Soc., Faraday Trans. 1*, *85* (3) (1989) 503; (c) L. Lauermann, D. Meissner and R. Memming, *J. Electroanal. Chem.*, *228* (1987) 45.
[7] S.B. Li, *French–Chinese Symposium on Catalysis, September, 1990, IFP, Rueil-Malmaison.*
[8] Y.G. He, S.Y. Yi, Q.L. Li and S.B. Li, *Photographic Science and Photochemistry*, *4* (1986) 51 (in Chinese).
[9] Q.L. Li, K.R. Sun, Y.G. He, S.B. Li and Z.S. Jin, *Acta Energiae Solaris Sinica*, *7* (2) (1986) 197.
[10] (a) Q.L. Li, B.M. Su, X.H. Zheng, K.B. Sun and Z.S. Jin, *Photographic Science and Photochemistry*, *31* (1986) 55 (in Chinese); (b) S.B. Li, *J. Molecular Catalysis (China)*, *2* (4) (1988) 217.
[11] E. Borgarello, N. Serpone, M. Pelizzetti and M. Barbeni, *J. Photochem.*, *33* (1986) 35–48.
[12] N. Buhler, K. Meier and J.-F. Reber, *J. Phys. Chem.*, *88* (1984) 3261.
[13] R.B. Heslop and K. Jones, *Inorganic Chemistry*, Elsevier Scientific Publishing Company, 1976, Chapter 39.
[14] R. Hayes, P.A. Freeman, P. Mulvaney, F. Grieser and T.W. Healy, *Ber. Bunsenges. Phys. Chem.*, *91* (1987) 231.
[15] D. Briggs (ed.), *Handbook of X-Ray and Ultraviolet Photoelectron Spectroscopy*, Heyden and Son Ltd., 1977.
[16] C.D. Wagner, W.M. Riggs and L.E. Davis, *Handbook of X-Ray Photoelectron Spectroscopy*, Perkin-Elemer Corporation, MN, 1978.
[17] L.M. Lehn, J.P. Sauvage and Z. Ziessel, *Nouv. J. Chim.*, *4* (1980) 623.
[18] A.R. West, *Solid Chemistry and Its Applications*, Wiley, 1984, Chapter 7.